Antiferromagnetic Resonance in MnO:Co: A Measurement of the Magnetoelastic Properties of the Co^{2+} Ion*

A. E. Hughes†
Laboratory of Atomic and Solid State Physics, Cornell University, Ithaca, New York 14850

(Received 22 June 1970)

The "out-of-plane" antiferromagnetic resonance frequency ω_1 of MnO has been followed as a function of Co-impurity concentration in the range 0.5–6.0 mole%. Using far-infrared techniques, ω_1 is observed to shift from 27.7 cm^{-1} in pure MnO to 38.0 cm^{-1} for 6.0% Co doping. Line broadening precluded the possibility of following the resonance to higher impurity concentrations. Measurements of ω_1 as a function of temperature confirm the magnetic nature of the resonance absorption lines, and are consistent with existing data which show that the Néel temperature of the mixed system is a linear function of impurity concentration. The perpendicular susceptibility, on the other hand, appears to change very little as Co is added to MnO. The square of the frequency ω_1 is found to be proportional to the Co concentration, suggesting that Co^{2+} single-ion anisotropy is primarily responsible for the shift, and an anisotropy contribution of 32.8 cm^{-1}/ion is deduced from the results. The theory of the magnetostriction of CoO developed by Kanamori is modified to deal with the present case, and it is shown that the observed anisotropy can be readily understood in these terms. The relevance of this result to the properties of CoO is discussed, in particular, the problem of magnetic anisotropy and the possibility of a dynamic Jahn-Teller effect in the paramagnetic state. Some features of antiferromagnetic resonance (AFMR) and anisotropy in doped antiferromagnets relevant to the interpretation of the experimental results are developed in two appendixes.

I. INTRODUCTION

The face-centered-cubic oxide antiferromagnets form an interesting group of materials, since, although they were among the first antiferromagnets to be studied both experimentally and theoretically, many of their properties remain imperfectly understood. In this paper we present measurements of antiferromagnetic resonance (AFMR) in MnO doped with Co, which demonstrate some of the resonance properties of doped antiferromagnets, and also indicate how the Co ion behaves magnetically in an octahedral environment.

The magnetic structure of MnO is well known, and is type-2 ordering for the fcc structure. The spin magnetic moment of Mn^{2+} ($S=\frac{5}{2}$) lies in the (111) plane, all spins in a given (111) plane being parallel, and antiparallel to the spins on adjacent (111) planes. The direction of the spins within each (111) plane has not been definitely established, but in the analogous NiO structure, the spins have been shown to lie in directions of the type $\langle 1\bar{1}2\rangle$.[1–3] It is highly probable that the same is true in MnO,[3] and we shall assume this to be the case. The AFMR behavior of these materials has been discussed by Keffer and O'Sullivan.[4] Unlike uniaxial antiferromagnets such as MnF_2, there are two different anisotropy fields which are important in the oxides. The spins are confined to the (111) plane by a relatively strong dipolar anisotropy energy K_1 (of order 10^7 erg/cm^3), and the spin direction within the plane is determined by a much smaller anisotropy energy[4] of about 10^5 erg/cm^3. Defining the spin direction $[1\bar{1}2]$ as the z axis and the [111] axis as the x axis, the anisotropy energy for small deviations from equilibrium can be written[4]

$$E_A=\tfrac{3}{4}K_1[\tfrac{1}{2}(\alpha_1^2+\alpha_2^2)-\alpha_1\alpha_2]+\tfrac{9}{2}K_2(\beta_1^2+\beta_2^2)+K_3\beta_1\beta_2. \quad (1)$$

K_2 and K_3 are "in-plane" anisotropy energies, and α, β, γ are direction cosines. There are then two resonance frequencies given by[4]

$$\omega_1/\gamma=[3K_1/\chi_\perp]^{1/2}, \quad (2)$$

$$\omega_2/\gamma=[(18K_2-2K_3)/\chi_\perp]^{1/2}, \quad (3)$$

where $\chi_\perp$ is the perpendicular susceptibility.

The particular combination of anisotropy energies in (2) and (3) can be found by considering the approach of Kanamori and Tachiki,[5] who show that AFMR frequencies are given by $\omega/\gamma=(2K/\chi_\perp)^{1/2}$ where K is the anisotropy energy for deviations which leave the sublattices antiparallel, i.e., $\alpha_2=-\alpha_1=\alpha$, $\beta_1=-\beta_2=\beta$. Then

$$E_A=\tfrac{3}{2}K_1\alpha^2+(9K_2-K_3)\beta^2, \quad (4)$$

from which (2) and (3) follow for the two modes.

Sievers and Tinkham[6] have observed the mode ω_1 in the far infrared at 27.7 cm^{-1}. Using this frequency and the experimental value[7] of $\chi_\perp$ of 4.31×10^{-4} emu/cm^3 gives $K_1=1.24\times10^7$ erg/cm^3, which is to be compared with $K_1=1.54\times10^7$ erg/cm^3 calculated for the dipolar anisotropy.[4,6,8] Sievers and Tinkham[6] actually quote better agree-

ment, but their value for $\chi_\perp$ is somewhat higher than the presently accepted value given above. Also relevant are the neutron-scattering studies of Collins,[9] who obtains a best fit with $K_1 = 1.90 \times 10^7$ erg/cm^3. These experimental values of K_1, although not in perfect accord with each other, do show that the dipolar anisotropy energy is the principal contributor to K_1. The differences arise because of uncertainty in the appropriate exchange field ($H_E = M/\chi_\perp$) to insert in the expressions (2) and (3). However, we may conclude that the behavior of the mode ω_1 is fairly well understood.

Much less is known about ω_2. It has been predicted to be a few cm^{-1},[4] but has escaped detection. However, static measurements of the spin-flop field[3,7] and examination of the magnetic-field dependence[10], of the high-frequency mode ω_1 suggest that ω_2 is less than 2 cm^{-1}. This means that $(18K_2 - 2K_3) \lesssim 2\times10^5$ erg/cm^3. We shall have little to add about the mysteries of ω_2.

The magnetic structure of CoO has been the subject of some controversy. Roth[11] suggested that the ordering was again type 2, the actual magnetization direction being $[\bar{1}\bar{1}7]$, i.e., 11° 30′ to the [001] axis. This structure at first seemed inconsistent with the tetragonal distortion of CoO below the Néel temperature (292 °K), and van Laar[12] proposed an alternative multi-spin-axis structure in which tetragonal symmetry was retained. This situation was apparently resolved when Saito *et al.*[13] found that there is a small rhombohedral distortion superimposed on the main tetragonal distortion. Their results favor the single-axis structure proposed by Roth. Kanamori[14,15] has shown how these distortions below T_N can be understood on the basis of magnetostriction caused by the residual orbital angular momentum of the Co^{2+} ion.

Following Kanamori's work, Tachiki[16] calculated the AFMR frequencies for CoO, and experimental searches for these modes have been made in the far infrared by Milward[17] and Daniel and Cracknell.[18] Neutron-scattering data on phonons and magnons in CoO have also been reported by Sakurai *et al.*[19] Milward[17] found a resonance at 142 cm^{-1}, while Daniel and Cracknell[18] report lines at 216, 221, and 248 cm^{-1}. The neutron-scattering data[19] show two broad magnon branches at about 160 and 230 cm^{-1}, which are almost flat over the whole Brillouin zone. These could be associated with the lines seen in the far infrared, but as Daniel and Cracknell[18] have shown, there is considerable difficulty in presenting a unified interpretation. Certainly, very little information about the magnetic anisotropy of CoO can be gained from these results, and therefore there are very few data to compare with the theoretical treatment of the anisotropy as given, for example, by Kanamori.[14,15]

Since many of the possible contributions to the anisotropy of CoO are single-ion effects, we can expect roughly the same behavior of the Co^{2+} ion in CoO and in the similar lattice of MnO. Thus, by measuring the AFMR frequency of MnO doped with Co, we shall show that it is possible to extract the single-ion anisotropy of Co^{2+} in an octahedral environment, and to compare the measured anisotropy energy with the various calculated contributions. This technique, of course, is closely related to the measurement of Co single-ion anisotropy in various ferrimagnets, a subject with a long history.[20] However, the interpretation of the anisotropy is essentially different in the present case, and very relevant to the properties of CoO, particularly the magnetostriction.

The dynamic behavior of doped ferro-, ferri-, and antiferromagnets has become of considerable interest in the last few years,[21] following a long-standing activity in the analogous field of the vibrations of doped and disordered lattices.[22] AFMR is not a very sensitive probe into the details of the dynamics of doped antiferromagnets, since being a $k = 0$ or "uniform" mode, it is usually assumed to probe only the "average" behavior of the lattice. We shall examine more carefully the extent to which this simplification can be applied, and show that in the present case this average approach is justified.

II. EXPERIMENTAL DETAILS

A. Samples

Both single-crystal and powder samples of MnO:Co were used for this work. The single crystals were kindly supplied by Slack of General Electric. They comprised parts of boules grown by flame fusion, and contained up to 10% concentrations of Co. Some mixed crystals of MnO and CoO in the mixture ratio 25:75, 50:50, and 75:25 were provided by Smakula of MIT. These samples were remnants from work carried out on the restrahl spectra of oxide mixtures.[23] Unfortunately, it was found that the AFMR transition could not be followed for concentrations of Co in MnO of more than about 6%, due to line broadening, so the MIT crystals were not useful for this purpose and were not studied in detail.

Powder samples of Co-doped MnO were prepared by the method used by Bacon *et al.*[24] Carbonates of appropriate doping level were precipitated out of solutions of $MnSO_4 \cdot H_2O$ and $Co(NO_3)_2 \cdot 6H_2O$, and then heat treated in vacuum and argon at 400 °C to produce monoxides. All samples thus prepared showed clear powder x-ray lines characteristic of a single mixed monoxide. The powders were cold pressed into pellets of about 1-cm diameter and a few mm thickness, using a roughly 1:1 mixture of

TABLE I. Analyses of Samples used in AFMR Experiments.

Sample	Single crystal or powder	Intended value of Co concentration x	Measured value of x
GE6	Single crystal	0.03	0.019–0.021
GE7A	Single crystal	0.03	0.048–0.066
GE7B	Single crystal	0.03	0.015
GE8	Single crystal	0.01	0.010
A3	Powder	0.050	0.046
A4	Powder	0.040	0.038
A7	Powder	0.060	0.058
C1	Powder	0.005	0.005_5
C2	Powder	0.018	0.018
C3	Powder	0.025	0.026
C4	Powder	0.030	0.030
C5	Powder	0.035	0.036

monoxide and KBr to give a firm binding.

The GE single crystals and the powders were chemically analyzed by Dr. R. Skogerboe of the Materials Science Center at Cornell. The actual concentration of Co in the single crystals was found to be significantly different from that intended during growth, and in one case a large variation across the sample was found (GE7A: see Table I). The powders, on the other hand, were very close to the intended concentration of Co. A summary of the samples used is given in Table I. Analysis also showed that the samples varied in stoichiometry, all of them having an excess of oxygen to some degree. This is usual in MnO, and, in fact, all samples showed some far-infrared lines characteristic of a few percent precipitated Mn_3O_4 [25] and presumably Co-doped Mn_3O_4. These lines, which will not be discussed in detail in this paper, can be troublesome since for some concentrations of Co they obscure the true AFMR line.

Single crystals of CoO for comparative work were obtained from the Nakazumi Crystals Corp., Osaka, Japan, and a piece of a flame-fused boule was kindly made available by Sahagian of the Air Force Cambridge Laboratories. Since these samples were of different origin from those used by Milward[17] and Daniel and Cracknell,[18] some relevant results will be briefly reported in Sec. III.

B. Far-Infrared Experiments

Absorption spectra in the range 2–120 cm^{-1} were recorded using a lamellar grating interferometer coupled to a He^3-cooled Ge bolometer. The interferometer has been fully described by Nolt *et al.*,[26] and the He^3 bolometer by Drew and Sievers.[27] Using this instrument, it was possible to obtain a signal-to-noise ratio of about 100 in the region of principal interest around the MnO AFMR line at 27.7 cm^{-1}. The absorption coefficient for each sample was obtained by comparing its transmission spectrum with that of a "dummy" sample, usually either a crystal of CoO (which has no lines in the region of interest) or a pressed-powder pellet of KBr.

Measurements of the temperature dependence of the AFMR frequency were made using a rig in which the sample was held in a $\frac{1}{2}$-in.-diam. stainless-steel "light pipe" about 6 in. above the level of liquid He^4 in the cryostat (see Ref. 27 for a diagram of the He^3 detector cryostat). A heater was wound close to the sample, and the temperature monitored using a Pt resistor and an Allen Bradley 10 kΩ carbon resistor. Stable temperatures of ±0.3 °K were obtainable with this rig in the temperature range above 20 °K without using any feedback for temperature control. Below 20 °K, good control was difficult because the heater input was very small. This was not a serious drawback since it is only above about 30 °K that detectable changes in frequency occur.

Samples were always wedge shaped so as to eliminate interference fringes caused by multiple reflections at parallel faces. This can be a serious problem with thin single-crystal samples because of the relatively high refractive index at frequencies below the restrahl in these oxides. By detecting such fringes, the "static" dielectric constant of MnO was determined to be 17.9 ± 0.7 at 1.2 °K, in reasonable agreement with other estimates at various "low" frequencies.[28]

III. RESULTS

The spectrum of one of the MnO:Co single crystals in the region 5–60 cm^{-1} is shown in Fig. 1. The most prominent feature is the AFMR line at 29.2 cm^{-1}, shifted upwards in frequency from its position in pure MnO. The absorption coefficient at the peak of the AFMR line is underestimated by an appreciable factor, because the absorption at the peak was essentially complete (i.e., zero transmission). Measurements on a thinner sample showed that the integrated absorption in the AFMR line was about 26 cm^{-2}, comparable with that in pure MnO. The weaker lines at 6 and 7 cm^{-1}, and the broad band at 49 cm^{-1} appeared in all the samples, and have been shown to be due to Mn_3O_4 precipitates.[25] There was, in fact, a rough correlation between their strength in the single crystals and the Co concentration, but this is probably only because the problem of nonstoichiometry is worse in the growing of doped crystals.

The effect on the AFMR frequency of increasing Co concentration is shown in Fig. 2. The data shown refer to a series of powder samples with mole fraction x of CoO (i.e., the formula can be written $Mn_{1-x}Co_xO$). The AFMR line shifts to considerably higher frequencies and broadens as x

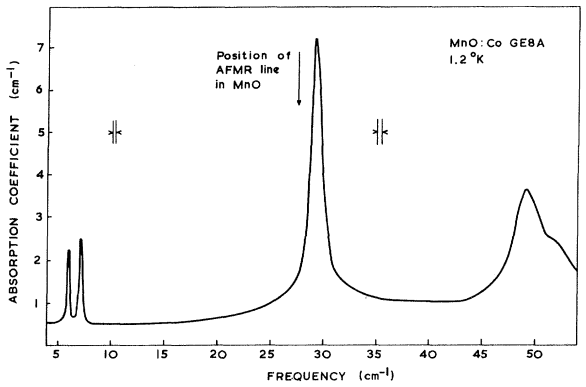

FIG. 1. Spectrum of MnO:Co ($x = 0.01$) at 1.2 °K in the range 5–60 cm^{-1}. The true absorption coefficient at the peak of the AFMR line at 29.2 cm^{-1} should be about 26 cm^{-1} (see text). The resolution of the spectrometer is indicated by the vertical bars.

increases. The linewidths observed in the powder samples were always somewhat larger than in the single crystals, but the trend is the same in both.

In order to confirm the magnetic nature of the transitions, the temperature dependence of the frequency was measured for two of the single crystals with $x = 0.01$ and 0.05. The results are shown in Fig. 3. As expected, the AFMR frequency drops sharply as the Néel temperature is approached and the linewidth increases. Measurement of the powder susceptibility of mixed MnO-CoO samples by Bacon *et al.*[24] showed that the Néel temperature varies linearly with x between $T_N = 116$ °K for MnO and $T_N = 292$ °K for CoO. The values of T_N, appropriate to our samples using this linear extrapolation, are shown by arrows in Fig. 3.

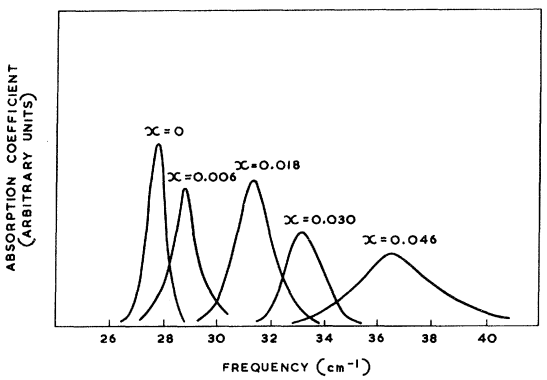

FIG. 2. AFMR absorption in MnO:Co as a function of Co concentration. Data were taken on various powder samples at either 1.2 or 4.2 °K, usually with a resolution of 0.4 cm^{-1}.

The temperature dependence of the AFMR frequency is seen to fit in well with this linear variation of T_N.

The temperature variation of the AFMR is principally determined by the temperature dependence of the anisotropy energy, since $\chi_\perp$ is nearly independent of temperature [see Eqs. (2) and (3)]. It is usually assumed that the anisotropy energy K behaves like some power of the sublattice magnetization,[29] the appropriate power law for K_1 being 2 on the molecular-field theory for dipolar anisotropy, or 3 on the Zener theory for an angular variation represented by a spherical harmonic of second order.[30,31] Sievers and Tinkham[6] have shown that in pure MnO (and NiO) the Zener theory gives the best fit, provided the square root of the elastic neutron-scattering intensity is taken to represent the sublattice magnetization M. This is because the Brillouin function for $S = \frac{5}{2}$ does not give a good representation of M, having too fast a temperature variation.[6]

Figure 4 shows the corresponding results for the doped samples, the data being normalized with respect to frequency and temperature. The lines represent the variation of $(K_1)^{1/2}$ as given by the molecular-field theory ($K_1 \propto M^2$) and the Zener theory ($K_1 \propto M^3$), where M is the sublattice magnetization of MnO. The Brillouin function for $S = \frac{5}{2}$ is also drawn for comparison with M. As for pure MnO,[6] the data fit the Zener theory best up to $T \sim 0.7 T_N$, after which the experimental points tend towards the molecular-field curve. Thus, even though the effective anisotropy energy is roughly double that of pure MnO for $x = 0.05$ (see below), the temperature dependence is described by the same variation of M, assuming the latter to be the same as in pure MnO. Thus, we conclude that the Co-induced anisotropy has a temperature variation very similar to that of pure MnO. Certainly, if the Co contribution varied according to a high power of M (e.g., M^{10} for cubic anisotropy[31]), then at least the $x = 0.05$ sample might be expected to show departures from the pure MnO behavior. It should be remembered, however, that the appropriate M for discussing the Co contribution may be that small part of the magnetization due to the Co ions themselves, which may have a different temperature dependence from that of the whole sublattice.[32] Nevertheless, a large difference in the appropriate power of the magnetization for the impurity and the host would make itself felt. This result will be discussed further in Sec. IV C.

We have already mentioned the relation between the AFMR frequency and the anisotropy energy. In order to make this identification for the doped system it is necessary to assume that we can use the average model for the uniform AFMR mode, in other words that we can write

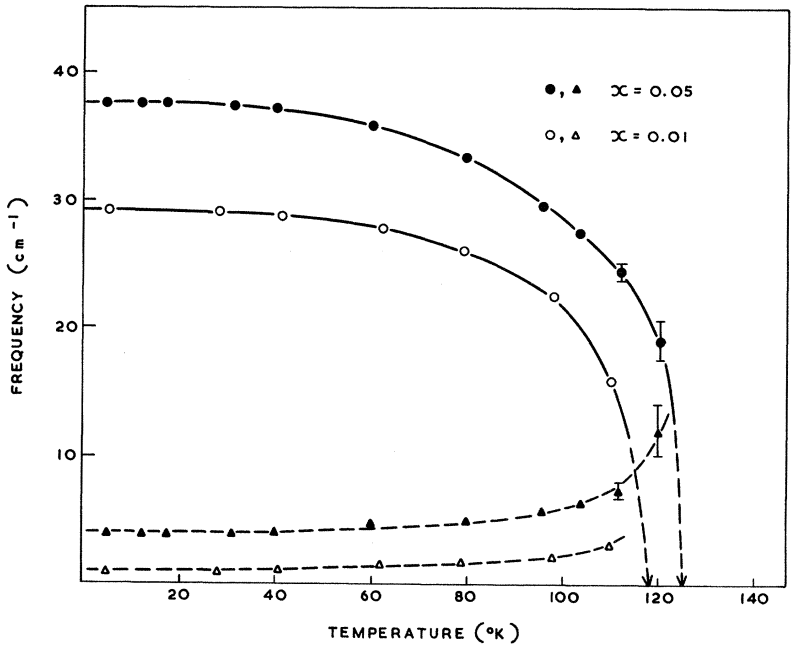

FIG. 3. Temperature dependence of the AFMR frequency in two single crystals of MnO : Co. The circles refer to the AFMR frequency and the triangles to the half-width of the absorption line. The arrows indicte the Néel temperatures deduced by linear extrapolation between MnO and CoO (see text).

$$\omega_1(x)/\gamma = [2K(x)/\chi_\perp(x)]^{1/2}, \qquad (5)$$

where K is now the relevant macroscopic anisotropy energy and $\chi_\perp$ the perpendicular susceptibility of the doped system. For the moment, we will assume this to be a valid approach; the justification is considered in Appendix A. It is then clear that a measurement of $\chi_\perp$ is imperative in order to extract the contribution of the Co ions to K. Fortunately, some measurements of the susceptibility of MnO-CoO mixtures have been made by Bacon *et al.*[24] They measured the powder susceptibility above and just below T_N for 25:75, 50:50, and 75:25 mixtures. These measurements have been extended to the concentration range $x = 0-0.05$,[33] and these results and those of Bacon *et al.* are shown in Fig. 5. The plotted susceptibility is that at T_N, which should be close to $\chi_\perp$. It was found difficult to get reliable values of χ at liquid-helium temperatures because of field-dependent hysteresis,[7] and also because there appeared to be ferro- or ferrimagnetic im-

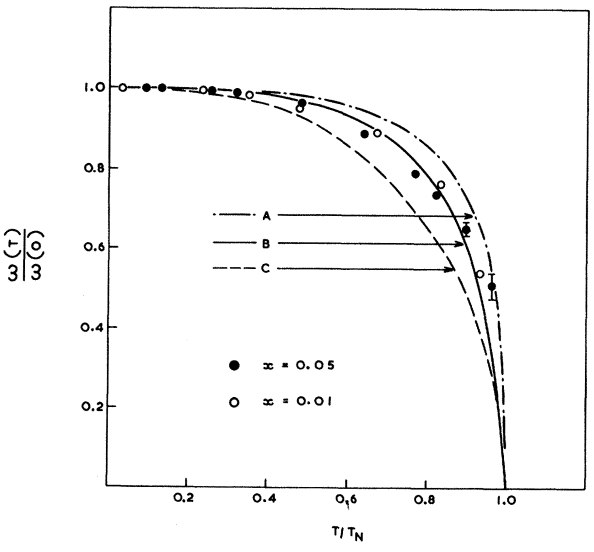

FIG. 4. Normalized temperature dependence of the AFMR frequency in MnO:Co. Curve A represents the molecular-field theory ($\omega \alpha M$), curve B the Zener theory ($\omega \alpha M^{3/2}$), and curve C is the Brillouin function for $S = \frac{5}{2}$. The sublattice magnetization M is taken as the square root of the neutron-scattering intensity (see Ref. 6).

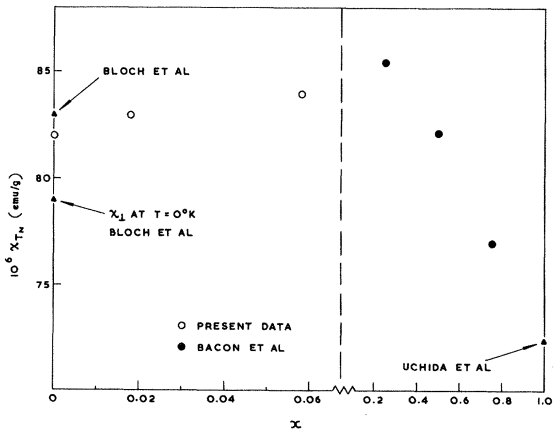

FIG. 5. Susceptibility at the Néel temperature of MnO : Co as a function of x. The full circles are the data of Bacon *et al.* (Ref. 24), and the triangles refer to the data on pure MnO and CoO of Bloch *et al.* (Ref. 7) and Uchida *et al.* (Ref. 36).

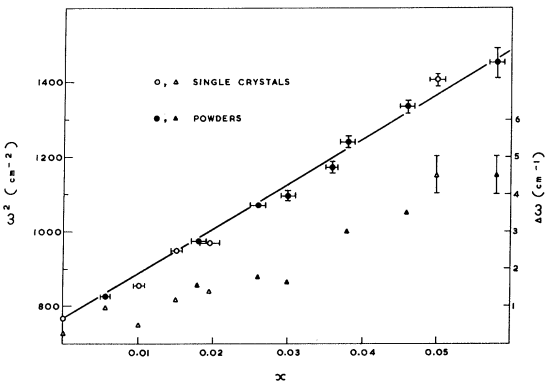

FIG. 6. The square of the AFMR frequency plotted as a function of x. The triangles and the scale on the right-hand ordinate refer to the half-width of the absorption line.

purities in the powder samples. These are probably the precipitates of Mn_3O_4 mentioned before. Figure 5 shows that χ_{T_N} (and, therefore, presumably $\chi_\perp$) varies very little with x, and thus we can regard $\omega_1(x)$ as measuring the anisotropy energy $K(x)$.

Equation (5) suggests that the meaningful quantity to plot is ω_1^2 vs x. This is shown in Fig. 6 for both single-crystal and powder samples. The half-width of the AFMR line is also plotted, although no attempt has been made to fit this to any specific model. The linearity of the ω_1^2-vs-x plot demonstrates that Co single-ion anisotropy is involved, as expected for reasons outlined in Sec. I. It is a little disturbing that the data depart from the least-squares-fit straight line by more than the limits of error. The probable explanation lies in the determination of x, since the accurate chemical analysis (as represented by the error bars) may not correspond exactly to the number of impurities *in solution* in the sample measured spectroscopically. Thus, we may accept the straight lines in Fig. 6 with some confidence and proceed to evaluate the contribution of each Co ion to the anisotropy energy.

To calculate the Co single-ion anisotropy, it is necessary to consider more carefully the form of $K(x)$. The form of the anisotropy energy for small spin deviations has been given in Eqs. (1) and (4) for pure MnO. Let us now assume that in the equilibrium situation the magnetic moment of the Co^{2+} ion is parallel to the spins of the Mn^{2+} ions on the same (111) plane. This is by no means obvious, since in CoO the predominant anisotropy energy is thought to be a magnetostrictive contribution of cubic symmetry,[15,29] which favors the [001] direction for the magnetic moment. In CoO the moment actually points in the $[\bar{1}\bar{1}7]$ direction[11] tilted towards the (111) plane by the trigonal component of the anisotropy (e.g., the dipolar terms). The angle between $[\bar{1}\bar{1}7]$ and [001] is 11° 31', whereas the direction of the Mn^{2+} spins in MnO $[\bar{1}\bar{1}2]$ makes an angle of 35° 18′ with [001]. Without knowing in advance the relevant anisotropy energies of Co^{2+} in MnO we cannot proceed any further, but it is shown in Appendix B that the assumption that the moments are in the same direction is a good representation of the situation.

Having temporarily sidestepped this problem, we can now write the anisotropy energy of the Co^{2+} ion for small deviations of the magnetic moment from equilibrium in the form

$$E_A(\mathrm{Co}) = k_a\alpha^2 + k_b\beta^2 \text{ (one ion)}, \tag{6}$$

where k_a, k_b represent the single-ion "out-of-plane" and "in-plane" anisotropy energies, respectively. For small concentrations of Co, we can neglect the change in the dipolar anisotropy K_1, since the moment of Co^{2+} in CoO ($3.8\mu_B$) is not too different from that of Mn^{2+} in MnO ($5\mu_B$). In any case, the dipolar anisotropy contributes at most a few cm^{-1}/ion to the anisotropy which will be shown to be negligible compared with the Co single-ion anisotropy. If there are N cation sites per cm^3 and a fraction x of Co, then there will be $xN/2$ Co^{2+} ions on each of the "up" and "down" sublattices. Thus, the total contribution of the Co ions to the anisotropy energy per cm^3 can be written

$$E_A(\mathrm{Co}) = xK_a[\tfrac{1}{2}(\alpha_1^2+\alpha_2^2)] + xK_b[\tfrac{1}{2}(\beta_1^2+\beta_2^2)], \tag{7}$$

where $K_a = Nk_a$, etc.

From Eqs. (1) and (7), the total effective anisotropy energy becomes

$$E_A = (\tfrac{3}{4}K_1 + xK_a)[\tfrac{1}{2}(\alpha_1^2+\alpha_2^2)] - \tfrac{3}{4}K_1\alpha_1\alpha_2 + (9K_2 + xK_b)[\tfrac{1}{2}(\beta_1^2+\beta_2^2)] + K_3\beta_1\beta_2. \tag{8}$$

The resonance frequencies are then

$$\omega_1(x)/\gamma = [(2/\chi_\perp)(\tfrac{3}{2}K_1 + xK_a)]^{1/2}, \tag{9}$$

$$\omega_2(x)/\gamma = [(2/\chi_\perp)(9K_2 - K_3 + xK_b)]^{1/2}. \tag{10}$$

The plot of $\omega_1^2(x)$ vs x thus gives K_a. Taking $\chi_\perp = 80\times10^{-6}$ emu/g(cf. for MnO $\chi_\perp = 79\times10^{-6}$ emu/g, Fig. 5) yields $K_a = (3.00\pm0.10)\times10^8$ erg/cm^3. Finally, since $N = 4.57\times10^{22}$, we find

$$k_a = 32.8\pm1.3 \text{ cm}^{-1} \text{ per } Co^{2+} \text{ ion}. \tag{11}$$

Equation (10) predicts that the in-plane mode ω_2 should also rise in frequency as x increases, and putting $k_b = k_a$ predicts $\omega_2(x) = 110x^{1/2}$ cm^{-1} if K_2 and K_3 are neglected. In this case, we would have $\omega_2 = 24.5$ cm^{-1} for $x = 0.05$ (e.g., sample GE7A). There is certainly no trace of a line in this region in GE7A, or indeed in any of the other samples of similar Co concentration. There is, however, some very complicated behavior in the 6–11-cm^{-1}

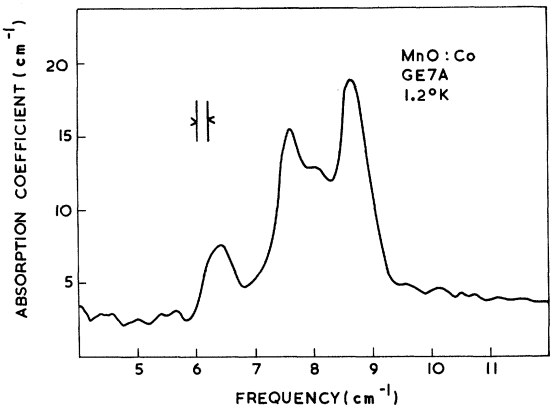

FIG. 7. Absorption spectrum of MnO : Co GE7A ($x = 0.05$) at 1.2 °K in the 6–11-cm^{-1} region. The spectrometer resolution is indicated by the vertical bars.

region in samples with $x > 0.015$, which is difficult to sort out because the Mn_3O_4 lines at 6 and 7 cm^{-1} are involved. The spectrum of GE7A in this region is shown in Fig. 7. It could be that somewhere among the chaos the in-plane mode ω_2 is playing its role. If this is the case, then we would have $k_b \sim 0.1 k_a$, which would be a little surprising if k_a is predominantly magnetostrictive in origin (see Sec. IV B). The lines in Fig. 7 all disappear above about 40 °K (the Curie temperature of Mn_3O_4 is 42 °K [34]). This does not necessarily rule out the possibility that one of them is due to ω_2, since the in-plane anisotropy energy might be expected to have a rapid temperature dependence in view of the sixfold in-plane symmetry.[4,6] The Zener theory predicts an M^{21} variation for the anisotropy constant in this case.[31] Nevertheless, we must admit that there is no real evidence for the observation of the in-plane mode in the doped samples.

In summary, the experimental results demonstrate the large effect on the anisotropy energy of doping MnO with Co. Provided we accept the simplifications made in interpreting the AFMR results on the basis of an average model, we derive a value of 32.8 ± 1.3 cm^{-1} for the Co single-ion anisotropy relevant to the out-of-plane mode ω_1. No definite results have emerged for the behavior of the in-plane mode. The interpretation of our results in terms of the magnetism of the Co^{2+} ion will be discussed in Sec. IV B.

Before concluding this section, we report briefly some measurements on CoO in the range 0–200 cm^{-1}. The data were obtained using a Michelson interferometer[35] with samples from two different sources, and the only absorption lines seen are shown in Fig. 8. Unfortunately, the higher-frequency range where Daniel and Cracknell[18] observed their lines could not be covered at the time of the experiment. The structure near 150 cm^{-1} is similar, but by no means identical, to the lines observed by Milward.[17] The total integrated absorption coefficient is small compared with that in the higher-frequency lines,[18] and Kramers-Kronig analysis shows that it only accounts for a contribution of 2×10^{-6} emu/g to $\chi_\perp$, compared with the measured value of 72×10^{-6} emu/g.[36] Either these transitions are intrinsic and relatively forbidden, or they are activated by impurities. The differences between the two samples measured here and the results of Milward argue in favor of an impurity effect; on the other hand, Sakurai *et al.*[19] do report a transition in this region in their neutron-scattering results which would fit in nicely with the observed lines. Obviously, more work is required on the far-infrared spectrum of CoO.

IV. DISCUSSION

A. Average Model for AFMR

The first points to consider are the validity of the simplifications in the interpretation introduced in Sec. III. Is the average model justified for AFMR in a mixed crystal, and to what extent are the results confused by the possibility that the local direction of the sublattice magnetization at and near a Co^{2+} ion is different from that in pure MnO? These two questions are considered in detail in the appendixes, and at this point we shall only state the conclusions reached there. Using a simple molecular-field model, it can be shown that the average model for AFMR works in the case where $\chi_\perp$ is independent of x. This is appropriate to the present case. Furthermore, it is possible to extend the molecular-field model to include crudely the effects of the orbital moment of an ion

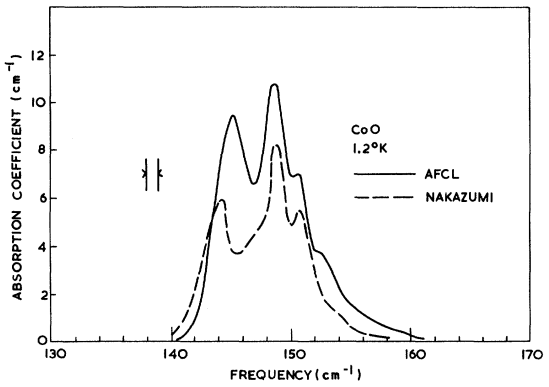

FIG. 8. Absorption lines near 150 cm^{-1} in two samples of CoO. Data were taken with a Michelson interferometer at 1.2 °K, with a resolution of 0.8 cm^{-1}. AFCL refers to a sample made available by Dr. Charles Sahagian of the Air Force Cambridge Laboratories, Bedford, Mass., and the other sample was supplied by the Nakazumi Crystals Corp., Osaka, Japan.

such as Co^{2+}. Provided that ω/γ for the AFMR is low compared with the exchange fields and the effective field due to the spin-orbit coupling energy, the spin and orbital moments of the Co^{2+} ions precess together with an effective gyromagnetic ratio γ_b, where

$$\frac{1}{\gamma_b}=\frac{m_l/\gamma_l+m_s/\gamma_s}{m_l+m_s}. \tag{12}$$

Here m_l, m_s are the orbital and spin components of the magnetic moment of the ground state. In a situation where $\chi_\perp$ is independent of x the AFMR frequency is then given by

$$\omega/\gamma_{eff}=(2K/\chi_\perp)^{1/2}, \tag{13}$$

where K is the mean anisotropy energy [e.g., Eq. (9)]. γ_{eff} is given by

$$\frac{1}{\gamma_{eff}^2}=\left(\frac{1-x}{\gamma_a^2}\right)+\frac{x}{\gamma_b^2}+x(1-x)\left(\frac{1}{\gamma_b}-\frac{1}{\gamma_a}\right)^2, \tag{14}$$

where γ_a is the gyromagnetic ratio of the Mn^{2+} ions and γ_b is given by Eq. (12). In the present case, the g factor involved in γ_{eff} changes from 2.0 for $x=0$ to about 1.9 for $x=0.05$, so there is no large error involved in using the value 2.0 in calculating the Co anisotropy, as we did in Sec. III.

The problem of local differences in the direction of sublattice magnetization is somewhat trickier. In Appendix B we present a simple linear chain model which suggests that a compromise is reached between the anisotropy energies and the exchange energies (as in a Bloch wall). The minority sublattices (Co in our case) point in some intermediate direction between their preferred equilibrium orientation and that of the majority sublattice. As one goes away from an impurity spin the host spins gradually tilt back towards their own preferred orientations. The small angle between neighboring spins thus costs some exchange energy, which is compensated by the reduction in anisotropy energy associated with having most of the spins fairly close to their preferred directions. The effective anisotropy energy of the whole system is then of the form $K(\delta\theta)^2$ where $(\delta\theta)$ represents a deviation of the whole system through an angle $\delta\theta$. In the simple model considered in Appendix B, K is given by the average of the anisotropy energies of each sublattice *referred to its own preferred direction*. Thus, even though canting does occur, the anisotropy energy due to an impurity refers to the preferred axis of the impurity magnetic moment. It is unfortunately possible that this conclusion does not strictly apply to Co in MnO, where the angular dependence of the anisotropy energies[15] is rather more complicated than those considered in the linear chain model. However, since the spins are always somewhere between the [001] axis and the $[\bar{1}\bar{1}2]$ axis, the angles involved are always fairly small ($< 35° = 0.6$ rad), and we may expect the representation of the anisotropy energies by effective fields, as done for the linear chain model, to be a reasonably good approximation.

In summary, the results of Appendixes A and B show that in the molecular-field scheme the simplifications that were made in interpreting the results of Sec. III are justified. There may well be departures from this simple model for MnO:Co, where orbital angular momentum and complicated angular dependence of the anisotropy energies are involved, but by and large the value derived for the Co^{2+} single-ion anisotropy energy can be taken as reliable. This allows us to go ahead and examine the interpretation of the results in terms of the electronic structure of the Co^{2+} ion.[14]

B. Co^{2+} Anisotropy Energy

The ground state of Co^{2+} in an octahedral crystal field is $^4T_1$. The threefold degenerate orbital state can be represented by an effective angular momentum $\vec{l}=1$, where $\vec{l}$ is related to the real angular-momentum operator $\vec{L}$ by $\vec{L}=-\alpha\vec{l}$. The constant α depends on the detailed structure of the $^4T_1$ state. In the weak-field case $^4T_1$ is wholly derived from ^4F of the free ion and $\alpha=1.5$. However, the octahedral crystal field mixes the ^4F and ^4P states of the Co^{2+} ion, which reduces α towards 1.0. In CoO, α is reduced to about 1.4,[14] so for all practical cases the mixing with ^4P can be neglected in discussing the anisotropy energies. The spin-orbit coupling energy can be written $\lambda\vec{L}\cdot\vec{S}$, λ in the free Co^{2+} ion being equal to -180 cm^{-1}.[14] Sakurai *et al.*[19] have suggested that in the paramagnetic state of CoO, λ is reduced to -71 cm^{-1}, possibly by the dynamic Jahn-Teller effect.[37] Most of the theoretical work on the ordered state of CoO has been done assuming $\lambda=-180$ cm^{-1}, and in Sec. IV D we will comment on the relevance of the anisotropy measurements to the problem of a Jahn-Teller effect in the paramagnetic state.

The first-order effect of the spin-orbit coupling gives no contribution to the anisotropy energy in octahedral symmetry.[15] This is to be contrasted with the usual situation in ferrites,[20] where Co^{2+} occupies a site of trigonal symmetry, which lifts the degeneracy of the T_1 orbital state into a lower doublet and a singlet about 1000 cm^{-1} higher. Within the doublet the spin-orbit coupling energy is anisotropic and it is this effect which is predominantly responsible for Co^{2+} single-ion anisotropy in spinels and garnets.[20,29] It could be argued that below the Néel temperature in MnO there is also a small trigonal distortion which might produce a similar source of anisotropy for a substituted Co^{2+} ion. However, the distortion corresponds to a

TABLE II. Sources of magnetic anisotropy other than magnetostriction in CoO [after Kanamori (Ref. 15)].

Mechanism	Contribution to anisotropy (cm^{-1}/ion) K	T
Interionic dipole-dipole	···	1.1
Intraionic spin-spin	0.78	···
Anisotropic spin-orbit interactions	2.00	···
Interionic orbital multipole interactions (Coulomb)	−11.1	···
Spin-independent direct exchange		$\lvert K\rvert, \lvert T\rvert \leq 4$, signs probably negative
Spin-independent direct exchange	···	$\lvert T\rvert \leq 3$, sign uncertain
Indirect exchange	~1–2	···

shear strain of about 10^{-3}, which would not be expected to split the T_1 orbital state by more than a few cm^{-1}. Thus, clearly in this case the effects of the spin-orbit coupling must be considered within the whole $^4T_1$ manifold.

The most complete analysis of the anisotropy energy of Co^{2+} in CoO is that due to Kanamori,[15,29,38] and we shall draw heavily on his work to discuss the similarities between CoO and Co^{2+} in MnO. With the exception of magnetoelastic contributions, which will be described in detail shortly, the various anisotropy contributions as calculated by Kanamori for CoO are given in Table II. The anisotropy energy is written in two parts, determined by symmetry considerations

$$E_A = K(\alpha^2\beta^2 + \beta^2\gamma^2 + \gamma^2\alpha^2) + T(\alpha\beta + \beta\gamma + \gamma\alpha). \quad (15)$$

Here α, β, γ are direction cosines of the magnetization relative to the cube axes. The K term is a cubic anisotropy term consistent with the octahedral symmetry of the Co site, and the T term has trigonal symmetry which reflects the trigonal symmetry of the spin arrangement in CoO (and MnO).[15] In general, single-ion effects contribute to the K term, and multiple-ion effects can contribute to both K and T. Competition between K and T is responsible for the $[\bar{1}\bar{1}7]$ orientation of the magnetization in CoO, since for positive K and $T = 0$ the cube axes are preferred, whereas for positive T and $K = 0$ the moment prefers the (111) plane. None of the sources of anisotropy in Table II are nearly as large as the value of 33 cm^{-1}/ion derived from the AFMR results in MnO: Co. In fact, the largest figure, that due to orbital multipole Coulomb interactions, cannot be nearly as large for Co in MnO as for CoO, since Mn^{2+} has an S ground state and therefore no multipole moments. Thus, although this contribution may be important in CoO (although it has the wrong sign to be the dominant effect[15]), it is irrelevant for Co as an impurity in MnO. The contributions listed in Table II can provide at most about 4 cm^{-1} per ion to both K and T in MnO: Co. It is worth noting that the dipole-dipole contribution to T is the one which in pure MnO is the major source of anisotropy.

Magnetoelastic effects provide the key to understanding the large anisotropy of Co in octahedral surroundings. The physical principle behind this effect is illustrated by Fig. 9. In a magnetic material the effective Hamiltonian for the ion can be written[14,29]

$$\mathcal{H} = g\mu_B \vec{S}\cdot\vec{H}_E + \lambda\vec{L}\cdot\vec{S}. \quad (16)$$

If $\vec{H}_E$ (the exchange field) is large, then the spin is forced to point along the direction of $\vec{H}_E$, and the spin-orbit coupling forces $\vec{L}$ to be parallel or antiparallel to $\vec{S}$, depending on the sign of λ. The orbital wave function is such that the electron density is nonspherical, and an asymmetric distortion of the lattice results. The energy involved in this distortion depends on the orientation of $\vec{L}$, and hence gives rise to magnetic anisotropy. The distortion is, of course, due to exactly the same forces which are responsible for Jahn-Teller effects in ions with orbital degeneracy, namely, interaction between lattice distortions and the orbital states.[37] The distinction between magnetostriction and the Jahn-Teller effect as usually discussed is simply a question of the order in which various effects are considered. In the example

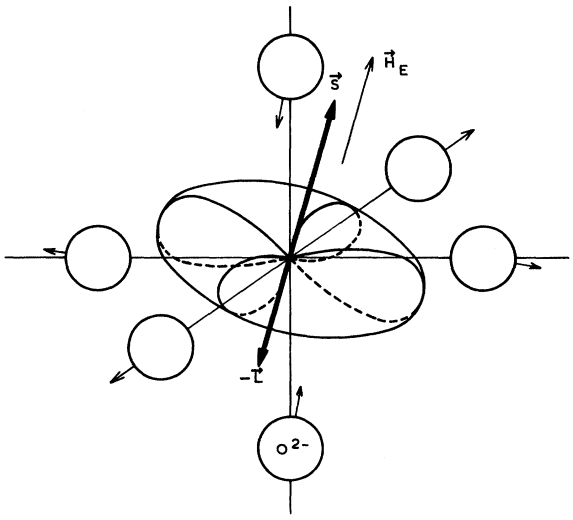

FIG. 9. Schematic representation of the mechanism of magnetostriction for an ion such as Co^{2+}. The exchange field $\vec{H}_E$ holds the spin in a particular direction, so that the spin-orbit coupling $\lambda\vec{L}\cdot\vec{S}$ forces the orbital angular momentum $\vec{L}$ parallel (or antiparallel, depending on the sign of λ) to the spin. The asymmetric charge density then results in a distortion of the lattice.

of magnetostriction represented by Fig. 9 the order of the energies is

Magnetic field (H_E) > spin orbit > distortion,

whereas in the usual treatment of the Jahn-Teller effect the order is precisely the opposite.

For Co^{2+} the situation is not quite as simple as in Fig. 9 because the two terms in $\mathcal{H}$ [Eq. (16)] are comparable (in CoO, [14] $g\mu_B H_E \sim 270$ cm^{-1}, $\lambda = -180$ cm^{-1}). The lowest eigenstate of $\mathcal{H}$ is then a linear combination of states from the $^4T_1$ manifold, which in terms of states $|S, l\rangle$ can be written (remembering that $\vec{L} = -1.5\vec{l}$)

$$|g\rangle = a|\tfrac{3}{2}, -1\rangle + b|\tfrac{1}{2}, 0\rangle + c|-\tfrac{1}{2}, +1\rangle. \quad (17)$$

The states are all quantized along the direction of H_E. Kanamori[14] finds that $a = 0.90$, $b = -0.4$, and $c = 0.17$. Thus, the ground state is composed mostly of the state of maximum spin, but the spin-orbit coupling mixes in states of reduced spin in the direction of H_E. Note that $\vec{l}$ is predominantly antiparallel to $\vec{S}$, so that $\vec{L}$ and $\vec{S}$ are parallel, as one would expect since λ is negative. Any distortion energy is now averaged over $|g\rangle$ rather than over $|\frac{3}{2}, -1\rangle$, otherwise the picture of the magnetostriction as given by Fig. 9 is the same. Magnetostriction is the source of the mainly tetragonal distortion observed in CoO below the Néel temperature, and the size of this distortion can be used to estimate the magnetostrictive coupling coefficients.

We shall now outline Kanamori's calculation of the magnetostriction of the Co ion. It is best to approach this initially from the point of view of CoO and then extend it to the case of Co as an impurity in MnO. Since the magnetostrictive coupling constants are predominantly between the Co^{2+} ion and its nearest neighbors, we expect them to be similar in the two cases. The only difference arises from the elastic forces resisting the deformation. In CoO the deformation is a bulk effect and therefore expressible in terms of the elastic constants of the crystal, whereas for Co in MnO the deformation is presumably local and it will be predominantly nearest-neighbor forces that are involved. We neglect for the moment the exchange striction which is responsible for the small rhombohedral distortions in CoO and MnO (this will be discussed later in this section), and consider only the energies resulting from coupling between the orbital components of the molecular-field ground state and the distortion of the lattice.

For a cubic crystal the magnetostrictive coupling energy can be written to lowest order in the direction cosines of the magnetization as[15,29]

$$E_{ME} = B_1[(\alpha^2 - \tfrac{1}{3})e_{xx} + (\beta^2 - \tfrac{1}{3})e_{yy} + (\gamma^2 - \tfrac{1}{3})e_{zz}] + B_2(\alpha\beta e_{xy} + \beta\gamma e_{yz} + \gamma\alpha e_{zx}). \quad (18)$$

Since the equilibrium strains will be a function of the direction cosines, E_{ME} represents an anisotropy energy. Writing the elastic energy of the crystal in the form

$$E_{elastic} = \tfrac{1}{2}c_{11}(e_{xx}^2 + e_{yy}^2 + e_{zz}^2) + c_{12}(e_{xx}e_{yy} + e_{yy}e_{zz} + e_{zz}e_{xx}) + \tfrac{1}{2}c_{44}(e_{xy}^2 + e_{yz}^2 + e_{zx}^2), \quad (19)$$

and minimizing $E_{ME} + E_{elastic}$ with respect to e_{ij}, the equilibrium values of the strain-tensor components are found to be[15,29]

$$e_{xx} = B_1(\tfrac{1}{3} - \alpha^2)/(c_{11} - c_{12}), \text{ etc.}, \quad (20)$$
$$e_{xy} = -B_2\alpha\beta/c_{44}, \text{ etc.}$$

Substituting these values for the strains in the expression for the total energy $E_{ME} + E_{elastic}$, we find that the distortion energy as a function of α, β, γ becomes

$$E_A = K_{ME}(\alpha^2\beta^2 + \beta^2\gamma^2 + \gamma^2\alpha^2) - B_1^2/3(c_{11} - c_{12}), \quad (22)$$

where

$$K_{ME} = B_1^2/(c_{11} - c_{12}) - B_2^2/2c_{44}. \quad (23)$$

For small deviations from the preferred [001] axis of K_{ME}, E_A may be written

$$E_A = K_{ME}\sin^2\theta, \quad (24)$$

where θ is the deviation of the magnetic moment. Equation (24) has the same form as Eq. (6) and we can therefore identify K_{ME} with k_a in our discussion of MnO: Co.

The calculation of the anisotropy due to magnetostriction involves a calculation of B_1 and B_2. B_1 and B_2 can be estimated from the observed distortion in CoO below T_N, or they can be calculated using a model of the crystal field and averaging the crystal-field energies over the molecular-field ground state of Co^{2+}. Kanamori has performed this kind of calculation using a point-ion model with both Slater[15] and Hartree[29,38] wave functions for the d orbitals of Co^{2+}. In comparing his calculations with experiment, he was forced to use the elastic constants of MgO since those of CoO were unavailable at the time. However, Sakurai *et al.*[19] have quoted the elastic constants of CoO, so we can use these in deriving experimental values of B_1 and B_2.

The tetragonal distortion in CoO extrapolated to 0 °K is estimated as $e_{zz} \approx -1.0 \times 10^{-2}$.[39] Inserting this value in Eq. (20) and using the elastic constants of CoO given by Sakurai *et al.*[19] (quoted accuracy 5–10%):

$$c_{11} = 3.1 \times 10^{12}, \quad c_{12} = 1.8 \times 10^{12},$$

$$c_{44} = 0.9 \times 10^{12} \text{ dyn/cm}^2,$$

we find $B_1 = 1.95 \times 10^{10}$ erg/cm^3, or 1900 cm^{-1}/ion. This can be compared with Kanamori's point-ion crystal-field values of 4.07×10^{10} erg/cm^3 (Slater

wave functions) and 2.5×10^{10} erg/cm^3 (Hartree wave functions). The small additional rhombohedral distortion is described by $e_{xy}=e_{yz}=e_{zx}=3\times10^{-4}$, and probably results predominantly from exchange striction rather than magnetostriction.[13] Kanamori's calculated value of B_2 is only 0.2×10^{10} erg/cm^3, which would predict $e_{xy}\sim-0.2\times10^{-4}$ and $e_{yz}=e_{zx}=1.4\times10^{-4}$. On the other hand, he has calculated $e_{xy}=e_{yz}=e_{zx}=-3\times10^{-4}$ for the exchange striction,[15] which is at least the right size even if the sign is wrong. The origin of the rhombohedral distortion is still uncertain,[13] but it is clear that B_2 must be much smaller than B_1. This merely means that the T_1 orbital wave functions interact more strongly with tetragonal than with trigonal distortions.

Combination of the magnetostrictive coefficient B_2 and the exchange striction (measured by a parameter B_3) produces a small trigonal anisotropy. The value of T is given by $-B_2B_3/c_{44}$.[15] Using Kanamori's value of B_2 and a value for B_3 consistent with the rhombohedral distortion ($e_{xy}=-B_3/c_{44}$) we find $T=6\times10^5$ erg/cm^3 or 0.07 cm^{-1}/ion. Thus, the effects of B_2 and B_3 can be safely ignored, and we may concentrate on the tetragonal parameter B_1.

As a first step towards calculating the magnetostrictive anisotropy of Co in MnO, let us see what the value of K_{ME} is expected to be in CoO. Using $B_1=1.95\times10^{10}$ erg/cm^3 and ignoring B_2, we find $K_{ME}=2.9\times10^8$ erg/cm^3, or 28 cm^{-1}/ion. This represents surprising agreement with the experimental measurement for Co in MnO, which was 32.8 cm^{-1}/ion (Sec. III). This is encouraging in view of our suggestion that the single-ion anisotropy of Co in MnO would be very similar to that of Co in CoO, and hence would throw some light on the magnetoelastic properties of the concentrated oxide. Let us now consider in more detail the case where Co^{2+} is an impurity.

The principal difference between Co in MnO and CoO is that presumably in the dilute case any magnetoelastic distortions are predominantly local. This means that the problem must be slightly reformulated to take account of this feature. It is possible that at high concentrations of Co in MnO some cooperative bulk distortion occurs (this happens in Co ferrites, for example),[29,38] but here we assume that the deformation around each ion is strongly localized, involving mainly the nearest neighbors.

Returning to Eq. (18) we now interpret the strains e_{ij} as local strains which represent the distortion of the octahedron of O^{2-} ions around the impurity. Since the lattice sums involved in calculating B_1 in Kanamori's point-ion theory fall off as R^{-3} and R^{-5}, it turns out that there is little error in confining the sums to the nearest neighbors.[15] Thus, we may take the value of B_1 for Co in CoO as also being representative for Co in MnO. Having determined the form of Eq. (18), an expression is now required which is analogous to Eq. (19) and represents the elastic forces opposing a distortion. This is a familiar problem in the analysis of the Jahn-Teller effect,[37] and we take a similar approach here. Since we are only considering terms in B_1, the relevant elastic energy is that for tetragonal distortions. Thus, we write

$$E_{\text{elastic}}=k_E[e_{zz}-\tfrac{1}{2}(e_{xx}+e_{yy})]^2+\tfrac{3}{4}k_E(e_{xx}-e_{yy})^2. \quad (25)$$

The combinations of strain components have been symmetry adapted to E_g-type modes. The force constant k_E remains to be determined.

Minimizing the total energy then gives $e_{xx}=B_1\times(\frac{1}{3}-\alpha^2)/3k_E$, etc. [cf. Eq. (20)] and therefore

$$K_{ME}=B_1^2/3k_E \quad . \quad (26)$$

All that remains is to identify k_E with some measurable quantity. We shall take the approach normally used in Jahn-Teller theory in which we express k_E in terms of a vibrational frequency ω for the octahedral cluster of O^{2-} ions. The elastic energy [Eq. (25)] can just as well be written in terms of the E_g-type normal modes of an octahedron, Q_θ and Q_ϵ, where Q_θ transforms like $2z^2-x^2-y^2$, etc. In this case

$$E_{\text{elastic}}=\tfrac{1}{2}\mu\omega^2(Q_\theta^2+Q_\epsilon^2), \quad (27)$$

and Q_θ, Q_ϵ can be normalized so that μ is the mass of O^{2-}. With this choice, Ham[40] has shown that Q_θ is related to the local strain $[e_{zz}-\frac{1}{2}(e_{xx}+e_{yy})]$ by

$$Q_\theta=(2R/\sqrt{3})[e_{zz}-\tfrac{1}{2}(e_{xx}+e_{yy})], \quad (28)$$

where R is the distance between the impurity and its nearest neighbors. It then follows that $3k_E=2\mu\omega^2R^2$. The frequency ω may at first sight seem as elusive as the force constant k_E, but, in fact, ω can in principle be determined from optical spectra of the impurity, since it is this frequency which broadens the optical absorption bands and can sometimes be observed as a definite phonon-assisted progression in the absorption spectrum. There is very limited information on the optical spectrum of Co^{2+} in CoO or MnO,[41] but in MgO[42] the transition from the ground $^4T_1$ state to the first excited state ($^4T_2$ derived from ^4F in the free ion) at 8500 cm^{-1} shows a progression involving a frequency of about 200 cm^{-1}. In any case, experience suggests that the effective ω is somewhere between the top of the acoustic band and the optical band of phonons, i.e., 200–400 cm^{-1} in both CoO and MnO.[19,43]

Assuming $\omega=200$ cm^{-1} and using the value of B_1 found for CoO (1900 cm^{-1}/ion) we calculate $K_{ME}=20$ cm^{-1}/ion. This again is in reasonable agreement with the measured value of 32.8 cm^{-1}/ion, although not as good as the previous estimate obtained by assuming that K_{ME} was the same for Co

in both CoO and MnO. Bearing in mind the fact that there may be nonmagnetoelastic contributions to both K and T of several cm^{-1}, we can nevertheless be satisfied that the physical origin of the large Co^{2+} single-ion anisotropy has been established. The value of K_{ME} is, of course, quite sensitive to the values of B_1 and ω. It can be raised to 30 cm^{-1} either by reducing ω to 165 cm^{-1}, or raising B_1 to 2370 cm^{-1}. Either of these adjustments is within the bounds of possibility. Accumulated errors (from the estimate of e_{zz} and the elastic constants) amount to at least $\pm 30\%$ since K_{ME} depends on the square of B_1.

The AFMR data on Co-doped MnO thus confirm that the dominant source of the anisotropy energy of Co in an octahedral site is magnetostrictive, and show that Kanamori's calculations provide a consistent model for the deformation and anisotropy of CoO. Previously, only the deformation could be used as a check on the theory, but we have now shown that the anisotropy energy of Co^{2+} is also largely accounted for with this mechanism. One point remaining, however, is the explanation of why the magnetic moment of CoO points in the $[\bar{1}\bar{1}7]$ direction rather than [001]. This requires T/K in Eq. (15) to be roughly $\frac{1}{3}$,[29] and having shown that K_{ME} is about 30 cm^{-1}, it would seem that we are left with the problem of finding something to contribute 10 cm^{-1} to T. In CoO, however, the total cubic anisotropy K may be reduced by as much as 12 cm^{-1} by the multipole interactions (Table II), and the required value of T may only be 6 cm^{-1}. The contributions listed in Table II may be sufficient to account for such a value. The multipole interactions are absent in MnO:Co, and therefore this system can be expected to provide a better measurement of the magnetostrictive anisotropy than CoO itself. It is possible, of course, that some contributions to T have been included in our measured value of K_a. For $T \ll K$, the effective anisotropy for small displacements $\delta\theta$ from the direction which makes Eq. (15) a minimum is given by $(K + T/2)(\delta\theta)^2$, so values of T of several cm^{-1} would not be out of line with our measurements.

C. Temperature Dependence

In Sec. III we discussed briefly the temperature dependence of the Co anisotropy, and suggested that K_a could not vary as a very high power of the sublattice magnetization. This is interesting because taken at face value the magnetostrictive anisotropy [Eq. (22)] involves fourth-order spherical harmonics, and hence on the Zener theory[30,31] might be expected to show an M^{10} variation with temperature, which seems too fast to be consistent with the data shown in Figs. 3 and 4. One way of getting around this problem is suggested by the situation in the rare-earth metals. Turov and Shavrov[44] suggested that in these materials the magnetoelastic anisotropy should be treated in the "frozen-lattice" configuration when discussing magnetic resonance. The idea here is that during resonance the lattice distortion cannot follow the precessing spins, so that the effective anisotropy energy is found by "freezing" the strains at their values corresponding to the equilibrium spin configuration, rather than letting the strains follow the motion of the spins. In deriving Eq. (22) by substituting Eqs. (20) and (21) in Eqs. (18) and (19) we have implicitly followed the latter course. In the frozen-lattice approach we should substitute the values of the strains at equilibrium in Eqs. (18) and (19), in other words

$$e_{xx} = B_1(\tfrac{1}{3} - \alpha_0^2)/(c_{11} - c_{12}) \tag{29}$$

rather than Eq. (20). If this is done, then the anisotropy energy becomes (ignoring B_2)

$$E_A = \frac{-B_1^2}{c_{11} - c_{12}} [(\tfrac{1}{3} - \alpha^2)(\tfrac{1}{3} - \alpha_0^2) + \cdots] + \text{const}, \tag{30}$$

which only involves second-order spherical harmonics and should behave like M^3 in the Zener theory. This is the same variation as found in pure MnO and may explain why the Co-induced anisotropy shows the same behavior, despite being attributed to an anisotropy energy of cubic symmetry. Note that E_A is still of the form in Eq. (24) for deviations from the [001] axis ($\gamma_0 = 1$). In the rare-earth metals Dy and Tb, the frozen-lattice model also gives the best fit to the temperature dependence of the anisotropy energies measured by ferromagnetic resonance.[45]

D. Jahn-Teller Effect in Paramagnetic State

We are now in a position to comment on the suggestion by Sakurai *et al.*[19] that in paramagnetic CoO the spin-orbit coupling constant λ is quenched from -180 to -71 cm^{-1} by a dynamic Jahn-Teller effect. Since the Jahn-Teller effect and magnetostriction are caused by the same type of coupling terms, it should be possible to make contact between them. To do this, it is most convenient to work for the most part in terms of local normal modes Q_θ, Q_ϵ, and from now on we shall do this assuming that this kind of "cluster model" is applicable to CoO as well as Co as an impurity in another host.

In Kanamori's theory of magnetostriction, the coupling between the orbital states of Co^{2+} (described by the effective angular momentum $\vec{l}$) and the strains can be written

$$\mathcal{H}_c = b_1[e_{xx} l_x^2 + e_{yy} l_y^2 + e_{zz} l_z^2 - \tfrac{2}{3}(e_{xx} + e_{yy} + e_{zz})] \tag{31}$$

[see Eq. (41) in Ref. 15], where we have not included e_{xy}, etc., since the B_2 term has been shown

to be negligible. The relation between b_1 and the magnetostrictive coefficient B_1 is

$$B_1 = \tfrac{1}{2}(a^2+c^2-2b^2)\,b_1\,, \tag{32}$$

where a, b, c are given by Eq. (17) and the factor $a^2+c^2-2b^2$ is about $\frac{1}{2}$ for CoO. Using the relation between Q_θ and $[e_{zz}-\frac{1}{2}(e_{xx}+e_{yy})]$ given in Eq. (28), and an analogous one for Q_ϵ, $\mathcal{H}_c$ can be transformed into

$$\mathcal{H}_c = [b_1/(\sqrt{3})R]\{[l_z^2-\tfrac{1}{2}(l_x^2+l_y^2)]Q_\theta + (\sqrt{3}/2)(l_x^2-l_y^2)Q_\epsilon\}\,. \tag{33}$$

This is now in the same form as the Jahn-Teller coupling Hamiltonian[37] conventionally used for a T_1 orbital state coupled to an E_g mode Q_θ, Q_ϵ, and serves to identify the Jahn-Teller energy E_{JT} as $b_1^2/6\mu\omega^2R^2$. E_{JT} does not in this case necessarily represent any particular energy shift, but is a useful parameter to measure the strength of the coupling represented by $\mathcal{H}_c$. Finally, using Eq. (32), we can quote the relation between E_{JT} and K_{ME}:

$$E_{JT} = \tfrac{16}{3}K_{ME} \simeq 180\ \text{cm}^{-1}. \tag{34}$$

At first sight this is very encouraging, since the quenching factor for λ given by the theory of the dynamic Jahn-Teller effect[37] will now be $e^{-3E_{JT}/2\hbar\omega}$, which is approximately $\frac{1}{3}$ with $\hbar\omega \simeq 200\ \text{cm}^{-1}$. This is not far off the factor suggested by Sakurai *et al.*, 71/180.[19] However, the use of this quenching factor will only apply if $2E_{JT} \gg |\lambda'|$ [37] ($\lambda' = -\alpha\lambda \simeq -1.5\lambda$, see Sec. IV B), which clearly does not hold in this case. In fact, if anything we should proceed from the opposite direction, and calculate the perturbing effects of $\mathcal{H}_c$ on the spin-orbit levels characterized by $\vec{j} = \vec{l} + \vec{S}$. This approach has been found useful by Ham *et al.*[46] in discussing the case of Fe^{2+} in MgO, and we can do the same kind of calculation for Co^{2+}. The principle behind the perturbation calculation is shown in Fig. 10(a). The spin-orbit coupling $\lambda'\vec{l}\cdot\vec{S}$ splits the ${}^4T_1$ state into three levels in first order (we neglect any higher-order spin-orbit effects), the states being described by $j = \frac{1}{2}$ (Γ_6), $\frac{3}{2}$ (Γ_8), and $\frac{5}{2}$ ($\Gamma_8+\Gamma_7$). The symbols in parentheses are group-theoretical labels for O_h. The energy separations are as shown for $\lambda = -180\ \text{cm}^{-1}$. For each electronic level there are, in zero order, a series of vibrational levels $n\hbar\omega$ above the electronic energy, where n is integral. The Hamiltonian $\mathcal{H}_c$ then couples the vibrational and electronic levels together, and since $\mathcal{H}_c$ is linear in Q, to order E_{JT} only states with $n=1$ are coupled to the purely electronic levels ($n=0$). The symmetry of an $n=1$ level is found by taking the product $\Gamma \times E$, where Γ is the irreducible representation of the electronic state corresponding to $n=0$. These levels are also shown in Fig. 10(a). The wave functions for each state can be constructed using tables of coupling coefficients for the cubic group,[47] and the perturbation calculation for the four $n=0$ levels carried through. The results are

$$j=\tfrac{1}{2}\quad E(\Gamma_6) = -E_{JT}\left(\frac{1}{10}\frac{\hbar\omega}{3\xi+\hbar\omega}+\frac{9}{10}\frac{\hbar\omega}{8\xi+\hbar\omega}\right),$$

$$j=\tfrac{3}{2}\quad E(\Gamma_8) = 3\xi - E_{JT}\left(\frac{8}{25}-\frac{1}{20}\frac{\hbar\omega}{3\xi-\hbar\omega}+\frac{63}{100}\frac{\hbar\omega}{5\xi+\hbar\omega}\right),$$

$$j=\tfrac{5}{2}\quad \begin{cases} E(\Gamma_7) = 8\xi - E_{JT}\left(\frac{1}{10}-\frac{9}{10}\frac{\hbar\omega}{5\xi-\hbar\omega}\right) \\ E(\Gamma_8) = 8\xi - E_{JT}\left(\frac{37}{100}-\frac{9}{20}\frac{\hbar\omega}{8\xi-\hbar\omega}-\frac{9}{50}\frac{\hbar\omega}{5\xi-\hbar\omega}\right), \end{cases}$$

where $\xi = \lambda'/2 = 135\ \text{cm}^{-1}$. The limits of validity of this approach are strictly $E_{JT} < \hbar\omega, \lambda'$, although Ham *et al.*[46] have shown that for Fe^{2+} the perturbation approach remains fairly accurate close to these limits. The present results for Co^{2+} are shown graphically in Fig. 10(b) for two values of $\hbar\omega$. Roughly the same kind of behavior is observed as for Fe^{2+},[46] in that the two lowest levels approach each other, but for no reasonable value of E_{JT} does the level structure approach that required by Sakurai *et al.*[19] ($E_{3/2}-E_{1/2} = 160\ \text{cm}^{-1}$, $E_{5/2}-E_{3/2} = 260\ \text{cm}^{-1}$).

Thus, we have the situation that there is a good explanation for the reduction in spin-orbit splitting if we blind ourselves to the fact that the inequality $2E_{JT} \gg \lambda'$ does not hold, but a poor result if we use the perturbation approach as above. Note that even arbitrarily making $E_{JT} \gg \lambda'$ does not help, because then the quenching will be too extreme unless $\hbar\omega$ is made unreasonably large. Undoubtedly, the reason for this dilemma lies in the fact that the effects of $\mathcal{H}_c$ and the spin-orbit coupling are comparable, and one should solve both problems together. We conjecture that if this could be done, then some effect similar to that required by Sakurai *et al.*[19] will result. The same argument can also be applied to the magnetostrictive calculation: In principle the exchange field, the spin-orbit coupling, and the magnetoelastic terms should be treated on the same footing, since they are all of similar size. In this case, however, treating the magnetoelastic terms as a first-order perturbation may be more trustworthy. The largest contributor to the ground state in Eq. (17) is the wave function $|\frac{3}{2}, -1\rangle$, and the next state above (at energy $\simeq \lambda' = 270\ \text{cm}^{-1}$) is mostly $|\frac{3}{2}, 0\rangle$. However, $\mathcal{H}_c$ does not couple these two states together, and therefore higher-order effects of $\mathcal{H}_c$ may not be important provided the coefficients b_1 and B_1 are not too large. The values implied by the measured anisotropy satisfy this criterion.

For Co^{2+} in MgO, $E_{3/2}-E_{1/2}$ is found to be 305 cm^{-1},[48] and the reduction from the value 405 cm^{-1}

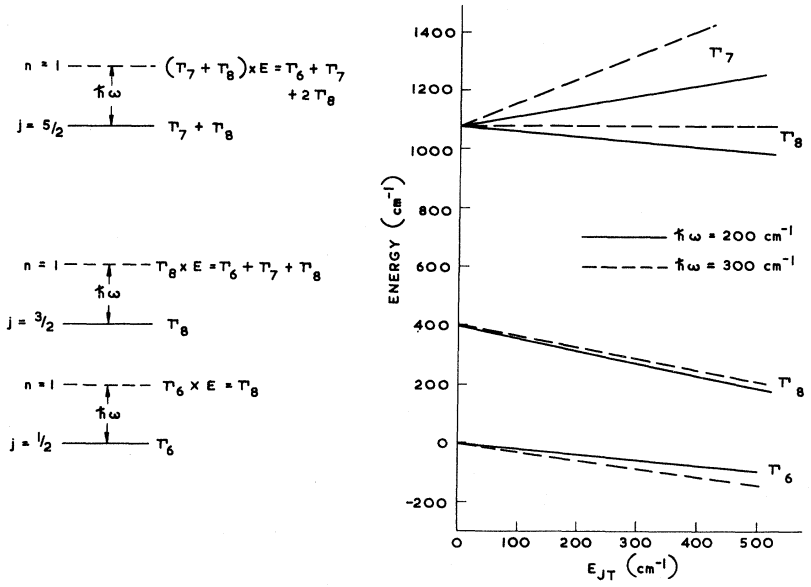

FIG. 10. (a) Group-theoretical labels for the symmetries of Co^{2+} levels in the coupling scheme for a perturbation calculation of the Jahn-Teller effect. The Γ's refer to the double-valued representations of O_h in the Bethe notation. (b) Variation of the $j=\frac{1}{2}$, $\frac{3}{2}$, and $\frac{5}{2}$ levels of (a) with Jahn-Teller energy, as calculated by perturbation theory. λ has been taken as -180 cm^{-1} (Ref. 14) and results are given for two values of the vibrational quantum $\hbar\omega$.

calculated using $\lambda = -180$ cm^{-1} can be explained in terms of covalent bonding.[49] The Jahn-Teller energy can be estimated from Tucker's [49] measured strain coupling coefficients, and is found to be ~ 110 cm^{-1}. Thus, it would appear that the Jahn-Teller coupling may be rather larger in CoO than in MgO.

V. SUMMARY

The AFMR frequency of MnO doped with Co has been shown to give a reliable measurement of the single-ion magnetic anisotropy of the Co^{2+} ion in octahedral coordination. Although there may be some open questions regarding the dynamics of AFMR in a mixed crystal, the models presented in the appendixes demonstrate that an interpretation in terms of average anisotropy energies is acceptable. Taking as a hypothesis the idea that Co^{2+} in MnO behaves rather similarly to Co^{2+} in CoO, the anisotropy has been interpreted as predominantly magnetostrictive in origin. Kanamori's calculations for the magnetostriction of CoO [15,38] have been adapted and shown to provide a good quantitative solution of the problem. The magnetostrictive coefficient B_1, which represents coupling to tetragonal distortions, dominates the anisotropy, and a value of B_1 consistent with the tetragonal deformation observed in CoO below the Néel temperature predicts closely the observed anisotropy energy of Co in MnO. In view of the temperature dependence of the AFMR frequencies, it is speculated that a frozen-lattice model[44,45] may be appropriate in describing the dynamical effects of magnetostriction.

The measurement of the magnetostrictive anisotropy leads naturally to an evaluation of the Jahn-Teller coupling of the $^4T_1$ state of Co^{2+} in the paramagnetic state of CoO. This predicts a Jahn-Teller energy of about 180 cm^{-1}, which while showing clearly that Jahn-Teller interactions are important in the paramagnetic state, nevertheless does not allow interpretation of the spin-orbit quenching observed by Sakurai *et al.* [19] in terms of simple Jahn-Teller models. The reason for this seems to be that Co^{2+} in CoO falls into the uncomfortable category of ions where Jahn-Teller and spin-orbit effects are comparable in magnitude, and should be treated together rather than dealing with one as a perturbation on the other. This type of Jahn-Teller problem is still basically unsolved in the dynamic regime, [37] and it remains to be shown whether or not such an approach can quantitatively explain the situation in CoO.

It was hoped at the outset that the results described in this paper would help to clear up the confusing situation of AFMR and spin waves in CoO. To some extent, this has been realized, since the analysis confirms quantitatively that the origins of magnetic anisotropy of Co in CoO must be predominantly magnetoelastic. Thus, the basis of calculations such as those of Ref. 16 for AFMR in CoO seems essentially correct, although the fact that the moment in CoO is in the $[\bar{1}\bar{1}7]$ direction rather than [001] may need to be taken into account. The conflicts of the experimental work on CoO by Milward, [17] Daniel and Cracknell, [18] and Sakurai *et al.*, [19] together with the limited work on CoO reported in this paper, nevertheless show that CoO is far from being satisfactorily understood. Much remains to be done in fully understanding this material, both in the ordered and paramagnetic phases, but perhaps the work reported here will be of use in providing quantitative data for further calculations. On

the other hand, we may be fairly satisfied that a happier state of affairs obtains for the AFMR and anisotropy properties of Co^{2+} as an impurity in MnO

Note added in proof. Some further work on the far-infrared spectrum of CoO has been reported by I. G. Austin and E. S. Garbett, [J. Phys. C 3, 1605 (1970)]. They observe a new resonance at 296 cm^{-1} in addition to lines similar to those observed previously.[17,18] Their results have some general features in common with the calculations of Alben,[16] but do not reproduce in detail the calculated intensities and temperature dependence.

ACKNOWLEDGMENTS

The author would like to thank Dr. G. A. Slack of General Electric, Professor A. Smakula of MIT, and Dr. Charles Sahagian of Air Force Cambridge Laboratories, all of whom made available samples which were used during this work. Also apppreciated is the value of discussions with Dr. Slack on the composition and properties of the crystals he supplied. A special debt of gratitude is owed to Professor A. J. Sievers and his group at Cornell for numerous relevant discussions, particularly those with Dr. R. Weber on the problem of resonance in doped magnetic materials. Finally, the author expresses his thanks to the Commonwealth Fund of New York for the award of a Harkness Fellowship.

APPENDIX A: ANTIFERROMAGNETIC RESONANCE IN MIXED SYSTEMS

Consider a simple two-sublattice antiferromagnet, where each sublattice has two types of magnetic ion a and b randomly dispersed in proportions $1-x$ and x. The sublattice magnetization of component a is written M_a and that of component b M_b, where these refer to unit volume. Thus, if the magnetization of a crystal composed wholly of species a is M, we have $M_a=(1-x)M$, etc. We now adopt a molecular-field model similar to that used by Bacon *et al.*,[24] and write the effective fields acting on each sublattice as

$$\begin{aligned}
\vec{H}_{1a} &= \vec{H}_a - \alpha_a \vec{M}_{2a} - \alpha_{ab}\vec{M}_{2b}\,,\\
\vec{H}_{1b} &= \vec{H}_b - \alpha_{ab}\vec{M}_{2a} - \alpha_b \vec{M}_{2b}\,,\\
\vec{H}_{2a} &= -\vec{H}_a - \alpha_a \vec{M}_{1a} - \alpha_{ab}\vec{M}_{1b}\,,\\
\vec{H}_{2b} &= -\vec{H}_b - \alpha_{ab}\vec{M}_{1a} - \alpha_b \vec{M}_{1b}\,.
\end{aligned} \tag{A1}$$

$\vec{H}_a$, $\vec{H}_b$ are anisotropy fields, α_a, α_b, α_{ab} are exchange constants, and 1 and 2 refer to an "up" and "down" sublattice, respectively.

Before discussing AFMR, let us consider the static properties of this model, and we temporarily neglect the anisotropy fields. First of all, by writing $\vec{M}_{1a}=C_a\vec{H}_{1a}/2T$, etc., where C_a is a Curie constant, the Néel temperature T_N may be found in the conventional way. In the special case $\alpha_{ab}^2=\alpha_a\alpha_b$ we find

$$T_N=(1-x)\,T_{Na}+x\,T_{Nb}\,, \tag{A2}$$

in an obvious notation. Bacon *et al.*[24] show that the relation $\alpha_{ab}^2=\alpha_a\alpha_b$ might be expected on the theory of superexchange, and their measurements on the MnO: CoO system confirm Eq. (A2).

The susceptibility at 0 °K, $\chi_\perp$, may be worked out by finding the equilibrium orientation of each sublattice subjected to the molecular fields in Eq. (A1) and an external field. The general result is quite complicated, but only if $\alpha_a=\alpha_b=\alpha_{ab}=\alpha$ does $\chi_\perp$ become independent of x, and then $\chi_\perp=1/\alpha$. This further restriction on the α's still satisfies $\alpha_{ab}^2=\alpha_a\alpha_b$. Since for MnO: CoO, $\chi_\perp$ is measured to be more or less independent of x, we take the approximation of putting all the exchange constants equal as being representative of this system as far as our simplified model is concerned. This conclusion will have to be modified when we consider orbital effects later in this section. If all the α's are equal, then it is also straightforward to show that $\chi(T_N)=\chi_\perp=1/\alpha$.

Let us now consider antiferromagnetic resonance in the mixed system. Using the effective fields in Eq. (A1), the equations of motion for each sublattice are (with $M^+=M_x+iM_y$):

$$\begin{aligned}
(1/i\gamma_a)\dot{M}_{1a}^+ &= -(H_a+\alpha_a M_a+\alpha_{ab}M_b)M_{1a}^+\\
&\quad -\alpha_a M_a M_{2a}^+ - \alpha_{ab}M_a M_{2b}^+\,,\\
(1/i\gamma_b)\dot{M}_{1b}^+ &= -(H_b+\alpha_b M_b+\alpha_{ab}M_a)M_{1b}^+\\
&\quad -\alpha_b M_b M_{2b}^+ - \alpha_{ab}M_b M_{2a}^+\,,
\end{aligned} \tag{A3}$$

with similar equations for $\dot{M}_{2a}^+$ and $\dot{M}_{2b}^+$. Taking the usual step of writing $d/dt=i\omega$, the resonance frequencies are then found as the roots of a 4×4 determinant. After some manipulation, in the simplest case $\alpha_a=\alpha_b=\alpha_{ab}=\alpha$, $\gamma_a=\gamma_b=\gamma$, the frequencies are found to be

$$\frac{\omega}{\gamma}=\alpha(M_a+M_b)+\left(\frac{M_bH_a+M_aH_b}{M_a+M_b}\right) \tag{A4}$$

and

$$\frac{\omega}{\gamma}=[2\alpha(M_aH_a+M_bH_b)]^{1/2}\,. \tag{A5}$$

To obtain the results in this form it is necessary to make the usual assumption that $H_a, H_b \ll \alpha(M_a+M_b)$.

The second frequency (A5) is seen to be in the usual AFMR form, especially if we write $H_a=K_a'/M_a$, etc., and $\chi_\perp=1/\alpha$ to get $\omega/\gamma=[(2/\chi_\perp)(K_a'+K_b')]^{1/2}$.

The physical significance of the first frequency is best seen by rewriting Eq. (A4) as

$$\frac{\omega}{\gamma}=\alpha(M_a+M_b)+H_b+\frac{M_b(H_a-H_b)}{M_a+M_b}\,. \tag{A6}$$

Thus, as $x \to 0$, $\omega/\gamma \to \alpha M_a + H_b$, which is the molecular-field frequency for a local mode involving single b-type ions in an a-type host.

This simple molecular-field model based on Eq. (A1) thus confirms the average model for AFMR in the case where $\chi_\perp = 1/\alpha$ is independent of x. We have not explored in detail the more formidable general problem that occurs when the exchange constants are not all equal.

It is of interest to see how the inclusion of an orbital moment as for Co^{2+} affects the equations of motion. Let us assume that the b component is Co^{2+}, and represent the spin magnetic moment *of one ion* by $\vec{m}_s$ and the orbital moment by $\vec{m}_l$. The spin-orbit coupling can be thought of as producing a term of the form $\eta \vec{m}_l \cdot \vec{m}_s$, so that the effective fields for the b *spin* sublattice become, in analogy to Eq. (A1),

$$\begin{aligned} \vec{H}_{1b}^{(s)} &= \vec{H}_b^{(s)} - \alpha_{ab}\vec{M}_{2a} - \alpha_b \vec{M}_{2b} - \eta \vec{m}_{1l} , \\ \vec{H}_{2b}^{(s)} &= -\vec{H}_b^{(s)} - \alpha_{ab}\vec{M}_{1a} - \alpha_b \vec{M}_{1b} - \eta \vec{m}_{2l} . \end{aligned} \tag{A7}$$

M_b now refers only to the spin component of the b sublattice magnetization, and $\vec{m}_{1s}$, $\vec{m}_{1l}$ refer to an ion on sublattice 1, etc. We assume implicitly that η is negative, so that $\vec{m}_l$ and $\vec{m}_s$ tend to be parallel. The equation of motion for M_{1b}^+ is then

$$\begin{aligned} (\omega/\gamma_s) M_{1b}^+ = &-(H_b^{(s)} + \alpha_{ab}M_a + \alpha_b M_b - \eta m_l) M_{1b}^+ \\ &- \alpha_{ab} M_b M_{2a}^+ - \alpha_b M_b M_{2b}^+ - \eta M_b m_{1l}^+ . \end{aligned} \tag{A8}$$

The effective field acting on $\vec{m}_{1l}$ can now be written, assuming an "anisotropy field" H_l for the orbital moment,

$$\vec{H}_{1b}^{(l)} = \vec{H}_l - \eta \vec{m}_{1s} . \tag{A9}$$

Thus, the equation of motion for m_{1l}^+ is

$$(\omega/\gamma_l) m_{1l}^+ = -m_{1l}^+ (H_l - \eta m_s) - \eta m_l m_{1s}^+ , \tag{A10}$$

so that

$$m_{1l}^+ = \frac{\eta m_l m_{1s}^+}{\eta m_s - H_l - (\omega/\gamma_l)} . \tag{A11}$$

For an ion such as Co^{2+} with a large spin-orbit coupling, we expect the AFMR frequency ω and the anisotropy field H_l to satisfy the inequality ω/γ_l, $H_l \ll \eta m_s$. This is true in our case where $\omega \sim 30$ cm^{-1}, $\lambda = -180$ cm^{-1}, and $K_{ME} \sim 30$ cm^{-1}, see Sec. IV. It is thus legitimate to linearize Eq. (A11) to obtain

$$m_{1l}^+ \simeq \frac{m_{1s}^+}{m_s}\left[m_l + \frac{\omega}{\eta \gamma_l}\left(\frac{m_l}{m_s}\right) + \frac{H_l}{\eta}\left(\frac{m_l}{m_s}\right)\right] . \tag{A12}$$

This may be substituted in Eq. (A8) to give (remembering that $m_{1s}^+/m_s = M_{1b}^+/M_b$)

$$\begin{aligned} \omega M_{1b}^+ &\left(\frac{1}{\gamma_s} + \frac{m_l}{m_s}\frac{1}{\gamma_l}\right) \\ &= -\left[H_b^{(s)} + H_l\left(\frac{m_l}{m_s}\right) + \alpha_{ab}M_a + \alpha_b M_b\right] M_{1b}^+ \\ &\quad - \alpha_{ab} M_b M_{2a}^+ - \alpha_b M_b M_{2b}^+ . \end{aligned} \tag{A13}$$

Since the orbital moment will contribute to $\chi_\perp$, the condition that $\chi_\perp$ be independent of x is no longer equivalent to all the α's being equal. Including the orbital moment m_l and the coupling $\eta \vec{m}_l \cdot \vec{m}_s$ in the calculation of $\chi_\perp$, it is straightforward to show that $\chi_\perp$ is independent of x and equal to $1/\alpha$ if

$$\alpha_a = \alpha, \quad \alpha_b = \alpha(M_b'/M_b)^2, \quad \alpha_{ab} = \alpha(M_b'/M_b) , \tag{A14}$$

where $M_b' = [1 + (m_l/m_s)]M_b$. M_b' is, in fact, just the total magnetic moment of a b sublattice, spin-plus orbital. Substituting these values of the exchange constants into the equations of motion, we reproduce the situation considered before, namely, Eqs. (A3) with all α's equal, provided we replace M_b by M_b' wherever it occurs. The anisotropy field for the b system, H_b, is given by

$$H_b = H_b^{(s)} + (m_l/m_s) H_l , \tag{A15}$$

$$\frac{1}{\gamma_b} = \frac{m_l/\gamma_l + m_s/\gamma_s}{m_l + m_s} . \tag{A16}$$

The reason the equations of motion reduce to those for the spin-only case is simply that the approximation of large spin-orbit coupling between equations (A11) and (A12) is tantamount to assuming that $\vec{m}_l$ and $\vec{m}_s$ are held parallel by a large (negative) value of η. Then the total magnetic moment precesses with an effective gyromagnetic ratio γ_b given by Eq. (A16), and an anisotropy field H_b given by Eq. (A15). In the case of Co^{2+}, or course, the orbital "anisotropy field" H_l is the major contributor to the total anisotropy energy, since it is the orbital component which produces magnetostriction.

The AFMR frequency in the case $\gamma_a \neq \gamma_b$ can be shown to be given by

$$\omega/\gamma_{eff} = [(2/\chi_\perp)(K_a' + K_b')]^{1/2}, \tag{A17}$$

where

$$\frac{1}{\gamma_{eff}^2} = \frac{(1-x)}{\gamma_a^2} + \frac{x}{\gamma_b^2} + x(1-x)\left(\frac{1}{\gamma_a} - \frac{1}{\gamma_b}\right)^2 . \tag{A18}$$

Thus, provided the spin-orbit coupling is large enough, the only effects of the orbital moment are in K_b' and γ_{eff}.

In the molecular-field ground-state equation (17) for Co^{2+}, we find $m_s = 2.6\mu_B$ and $m_l = 1.2\mu_B$. With these values, γ_b corresponds to a g value of 1.52, and γ_{eff} departs from the spin-only value by less than 5% over the range of Co concentration used in

the experiments.

APPENDIX B: CANTING OF SPINS WHEN HOST AND IMPURITY ANISOTROPY FIELDS ARE NOT COLLINEAR

Consider a linear chain of $(N+1)$ "host" spins S with an impurity at each end, Fig. 11. For simplicity, we assume all nearest-neighbor exchange interactions are the same, and that the impurity also has spin S. Let the anisotropy energy of a host spin be $k_1\alpha^2$, where α is the deviation from an easy axis, and that of an impurity be $k_2(\beta-\theta)^2$. β is the angle made by the preferred direction z' of the impurity spin with that of a host spin, z. We assume that in any canting that occurs the angle between adjacent spins is a constant ϕ. Then for the host spins we have

$$\alpha_n = \alpha_0 + |n|\phi, \tag{B1}$$

where $\alpha_{N/2+1} = \theta$. Thus, the total host anisotropy energy is

$$E_1 = k_1 \sum_{n=-N/2}^{N/2} (\alpha_0 + |n|\phi)^2. \tag{B2}$$

Since $\alpha_0 = \theta - (N/2+1)\,\phi$, we find for $N \gg 1$:

$$E_1 = k_1(N\theta^2 + \tfrac{1}{12}N^3\phi^2 - \tfrac{1}{2}N^2\theta\phi). \tag{B3}$$

The impurity anisotropy is given by

$$E_2 = k_2(\beta-\theta)^2, \tag{B4}$$

where we assume one impurity is effective for each chain, since we imagine the chains continued through a "lattice". The total exchange energy is (for $N \gg 1$)

$$E_J = NJS^2\phi^2 - 2NJS^2. \tag{B5}$$

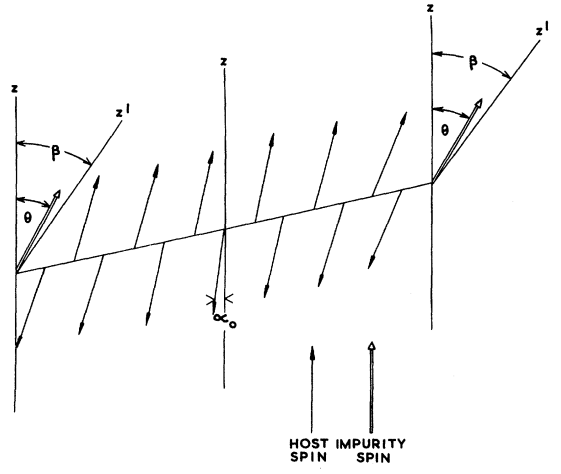

FIG. 11. Linear chain of host spins with impurities at both ends. z is the preferred direction for the host spins and z' that for the impurity spins. α_0 is the deviation for the host spin in the middle of the chain.

Taking $\partial E/\partial\theta = \partial E/\partial\phi = 0$, where $E = E_1 + E_2 + E_J$, we find

$$\phi/\theta = 3Nk_1/(12JS^2 + N^2k_1), \tag{B6}$$

$$\theta = \beta\left(1 + \frac{Nk_1}{k_2} - \frac{3N^3k_1^2}{4k_2(12JS^2 + N^2k_1)}\right)^{-1}. \tag{B7}$$

For N very large $N^2k_1 \gg 12JS^2$, and we have the simplification

$$\phi/\theta = 3/N, \quad \theta = \beta(1 + Nk_1/4k_2)^{-1}. \tag{B8}$$

This result can only be very approximate since it predicts $\alpha_0 < 0$, but (B8) shows roughly what can be expected to happen. The impurity spin tilts to some finite value of θ to approach its preferred direction $\theta = \beta$, while the host spins successively point closer and closer to their preferred direction $\alpha = 0$ as one goes further away from the impurity. The actual value of θ depends on k_1 and k_2.

The effective anisotropy energy of the whole chain is given by $K = \frac{1}{2}(\partial^2 E/\partial\theta^2)_{\min}$. From Eqs. (B3)–(B5), we clearly have

$$K = Nk_1 + k_2, \tag{B9}$$

so the anisotropy energy is the same as if the spins all pointed in their preferred directions.

It is instructive to put some numbers into Eqs. (B6) and (B7) to see what the angles are likely to be for a system like MnO: Co. Writing

$$k_1 = SH_{A1}, \quad k_2 = SH_{A2}, \quad J = H_E/S,$$

where H_{A1}, H_{A2}, and H_E are anisotropy and exchange fields, we have the following representative values for MnO: Co:

$$H_{A1} \approx 3\times10^4 \text{ Oe}, \quad H_{A2} \approx 20H_{A1} \approx 6\times10^5 \text{ Oe},$$

$$H_E \approx 10^6 \text{ Oe}, \tag{B10}$$

and we take $N = 20$ to represent 5% of Co impurity. Then we find $\phi/\theta \approx 0.075$, and $\theta \approx 0.7\beta$. Thus, the Co moment is about three-fourths of the way towards its preferred direction, and the Mn spin at the center of the chain is tilted away from its preferred direction by $\alpha_0 \approx 0.2\beta$.

These calculations must be regarded as crude, since in the fcc structure the anisotropy energies are more complex angular functions than we have assumed here [e.g., see Eq. (15) in the text]. This will have the effect of making K in Eq. (B9) no longer simply linear in N, i.e., K will no longer simply be an average of the individual anisotropy energies. Nevertheless, the angles of deviation from preferred axes in the MnO: Co system are fairly small (30° at the most), and the small-angle approximation of making anisotropy energies quadratic in the angle of deviation is not too bad. Then we can expect (B9) to be a reasonably good guide to the situation.

*Work supported by the Advanced Research Projects Agency, through the Materials Science Center at Cornell University, Report No. 1348.

†Present address: Solid State Division, Atomic Energy Research Establishment, Harwell, Didcot, Berkshire, England. The work at Cornell was done during the tenure of a Harkness Fellowship of the Commonwealth Fund of New York.

[1]T. Yamada, J. Phys. Soc. Japan 21, 664 (1966).

[2]T. Yamada, S. Saito, and Y. Shimomura, J. Phys. Soc. Japan 21, 672 (1966).

[3]E. Uchida, N. Fukuoka, H. Kondoh, T. Takeda, Y. Nakazumi, and T. Nagamiya, J. Phys. Soc. Japan 23, 1197 (1967).

[4]F. Keffer and W. O'Sullivan, Phys. Rev. 108, 637 (1957).

[5]J. Kanamori and M. Tachiki, J. Phys. Soc. Japan 17, 1384 (1962).

[6]A. J. Sievers and M. Tinkham, Phys. Rev. 129, 1566 (1963).

[7]D. Bloch, J. L. Feron, R. Georges, and I. S. Jacobs, J. Appl. Phys. 38, 1474 (1967).

[8]J. I. Kaplan, J. Chem. Phys. 22, 1709 (1954).

[9]M. F. Collins, in *Proceedings of the International Conference on Magnetism* (The Institute of Physics and Physical Society, London, 1964), p. 319.

[10]A. E. Hughes, *High Magnetic Fields and their Applications* (The Institute of Physics and Physical Society, London, 1969), p. 110.

[11]W. L. Roth, Phys. Rev. 110, 1333 (1958).

[12]B. van Laar, Phys. Rev. 138, A584 (1965).

[13]S. Saito, K. Nakahigashi, and Y. Shimomura, J. Phys. Soc. Japan 21, 850 (1966).

[14]J. Kanamori, Progr. Theoret. Phys. (Kyoto), 17, 177 (1957).

[15]J. Kanamori, Progr. Theoret. Phys. (Kyoto), 17, 197 (1957).

[16]M. Tachiki, J. Phys. Soc. Japan 19, 454 (1964). See also, R. Alben, J. Appl. Phys. 40, 1112 (1969); Phys. Rev. 184, 495 (1969).

[17]R. C. Milward, Phys. Letters 16, 244 (1965).

[18]M. R. Daniel and A. P. Cracknell, Phys. Rev. 177, 932 (1969).

[19]J. Sakurai, W. J. L. Buyers, R. A. Cowley, and G. Dolling, Phys. Rev. 167, 510 (1968).

[20]See, for example, R. F. Pearson, J. Appl. Phys. 31, 160S (1960); L. R. Bickford, J. M. Brownlow, and R. F. Penoyer, Proc. IEEE Suppl. B104, 238 (1957); M. D. Sturge, E. M. Gyorgy, R. C. LeCraw, and J. P. Remeika, Phys. Rev. 180, 413 (1969).

[21]See, for example, D. Hone, H. Callen, and L. R. Walker, Phys. Rev. 144, 283 (1966); S. W. Lovesey, J. Phys. C 1, 102 (1968); 1, 118 (1968); R. Weber, Z. Physik 223, 299 (1969).

[22]For reviews, see A. A. Maradudin, in *Solid State Physics*, edited by F. Seitz and D. Turnbull (Academic, New York, 1966), Vol. 18, p. 273; Vol. 19, p. 1.

[23]P. J. Gielisse, J. N. Plendl, L. C. Mansur, R. Marshall, S. S. Mitra, R. Mykolajewycz, and A. Smakula, J. Appl. Phys. 36, 2446 (1965).

[24]G. E. Bacon, R. Street, and R. H. Tredgold, Proc. Roy. Soc. (London) A 217, 252 (1953).

[25]A. E. Hughes (unpublished); see also Ref. 10.

[26]I. G. Nolt, R. D. Kirby, C. D. Lytle, and A. J. Sievers, Appl. Opt. 8, 309 (1969).

[27]H. D. Drew and A. J. Sievers, Appl. Opt. 8, 2067 (1969).

[28]J. N. Plendl, L. C. Mansur, S. S. Mitra, and I. F. Chang, Solid State Commun. 7, 109 (1969); T. B. Kinney and M. O'Keefe, *ibid.* 7, 997 (1969); C. Crevecoeur and H. J. DeWit, *ibid.* 6, 843 (1968); A. K. Chaudhury and K. V. Rao, Phys. Status Solidi 32, 731 (1969).

[29]J. Kanamori, in *Magnetism*, edited by G. T. Rado and H. Suhl (Academic, New York, 1963), Vol. I, p. 127.

[30]C. Zener, Phys. Rev. 96, 1335 (1954).

[31]H. B. Callen and E. Callen, J. Phys. Chem. Solids 27, 1271 (1966).

[32]G. K. Wertheim, H. J. Guggenheim, and D. N. E. Buchanan, Phys. Rev. Letters 20, 1158 (1968).

[33]I am extremely grateful to Dr. W. E. Gardner and J. Penfold of Materials Physics Division, AERE, Harwell, for making these measurements.

[34]K. Dwight and N. Menyuk, Phys. Rev. 119, 1470 (1960).

[35]I am grateful to Dr. R. Weber for assistance with these experiments.

[36]E. Uchida, N. Fukuoka, H. Kondoh, T. Takeda, Y. Nakazumi, and T. Nagamiya, J. Phys. Soc. Japan 19, 2088 (1964).

[37]F. S. Ham, Phys. Rev. 138, A1727 (1965); M. D. Sturge, in *Solid State Physics*, edited by F. Seitz, D. Turnbull, and H. Ehrenreich (Academic, New York, 1967), Vol. 20, p. 92.

[38]J. Kanamori, J. Appl. Phys. Suppl. 31, 14 (1960).

[39]N. C. Tombs and H. P. Rooksby, Nature 165, 442 (1950). Kanamori (see Ref. 29) estimates $e_{zz}=0.8\times10^{-2}$ at 0 °K from Tombs and Rooksby's value of 0.77×10^{-2} at 93 °K. The temperature dependence of the tetragonal distortion of CoO calculated by Sakurai *et al.* (see Fig. 8 of Ref. 19) suggests that a somewhat higher value of e_{zz} might be appropriate, and we adopt 1.0×10^{-2}. The uncertainty is unfortunate, since the final result for K_{ME} depends on the square of the value chosen for e_{zz} [see Eqs. (22) and (23)].

[40]F. S. Ham, Phys. Rev. 166, 307 (1968).

[41]G. W. Pratt and R. Coelho, Phys. Rev. 116, 281 (1959); D. R. Huffman, J. Appl. Phys. 40, 1334 (1969).

[42]R. Pappalardo, D. L. Wood, and R. C. Linares, J. Chem. Phys. 35, 2041 (1961); J. E. Ralph and M. G. Townsend, *ibid.* 48, 149 (1968).

[43]B. C. G. Haywood and M. F. Collins, J. Phys. C 2, 46 (1969).

[44]E. A. Turov and V. G. Shavrov, Fiz. Tverd. Tela 7, 217 (1965) [Soviet Phys. Solid State 7, 166 (1965)].

[45]H. S. Marsh and A. J. Sievers, J. Appl. Phys. 40, 1563 (1969).

[46]F. S. Ham, W. M. Schwarz, and M. C. M. O'Brien, Phys. Rev. 185, 548 (1969).

[47]J. S. Griffith, *The Theory of Transition Metal Ions*, (Cambridge U. P., England, 1961); G. F. Koster, J. O. Dimmock, R. G. Wheeler, and H. Statz, *Properties of the Thirty-two Point Groups* (MIT Press, Cambridge, Mass., 1963).

[48]P. Cossee, Mol. Phys. 3, 125 (1960).

[49]D. J. I. Fry and P. M. Llewellyn (with appendix by M. H. L. Pryce), Proc. Roy. Soc. (London) A266, 84 (1962); E. B. Tucker, Phys. Rev. 143, 264 (1966).